



Petrogenesis and tectonic implications of Miocene dikes in the southeast of Bam (SE Iran): Constraints on the development of active continental margin

Shahrbanoo Ousta ¹, Afshin Ashja-Ardalan ^{1,*}, Abdollah Yazdi ^{2,*}, Rahim Dabiri ³,
Mohammad Ali Arian ¹

¹ Department of Geology, North Tehran Branch, Islamic Azad University, Tehran, Iran

² Department of Geology, Kahnoot Branch, Islamic Azad University, Kahnoot, Iran

³ Department of Geology, Mashhad Branch, Islamic Azad University, Mashhad, Iran

Received: 25 August 2023, Revised: 12 October 2023, Accepted: 21 October 2023

© University of Tehran

Abstract

Fudge dikes of diorite and microdiorite are penetrated in the Mio-Pliocene sedimentary-volcanic series in the northeast of Bam. In terms of lithology, these dikes are placed in two categories: gabbro-diorite. The primary minerals of the dikes are plagioclase, amphibole (hornblende), and augite, and secondary minerals such as chlorite, biotite, and sericite. Also, their textures are granular, ophitic, and microgranular. From the geochemical point of view, gabbro-diorites have sub-alkaline and met aluminum with enrichment of LILE and HREE and depletion of Nb and Ta elements. The parental magma of the gabbro-diorites is obtained from the melting of a part of the subcontinental lithospheric mantle affected by the subduction producers and in equilibrium with lherzolite spinel. The characteristics of incompatible element patterns include LILE enrichment and HFSE depletion compared to REE similar to subduction zone igneous rocks. These rocks show the intermediate geochemical characteristics of the volcanic arc magmatism of arc islands and margins, consistent with the formation of these rocks in active continents. Geochemical evidence, as well as the association of igneous rocks with green tuffites and other shallow sea sediments, indicate the occurrence of an extensional basin behind the continental arc.

Keywords: Swarm Dike, Extensional Basin, Miocene, Southeast Bam.

Introduction

Fudge dikes (Dike Swarm) are a group of parallel, linear, or radial dikes that can be observed in a range of several tens of kilometers to several thousand kilometers in various geological environments. Dike masses are commonly associated with divergent continental margins, particularly large igneous provinces, and continental breakup (Ernst et al., 1996; Goldberg, 2010; Ernst, 2014). and are related to mantle columns (Fahrig, 1987). Fudge dikes primarily form as a result of magma rising through fractures generated by regional tensile stresses or volcanic rifts (Kjoll et al., 2019; Ernest et al., 1995). These dikes are regarded as valuable tools for discerning the positions of mantle plumes, the orientation and movement of tectonic boundaries, the evolution of various patterns over time, and other related phenomena.

An important issue that should be taken into account is that the formation of ophiolites in the

* Corresponding author e-mail: afshinashjaardalan@yahoo.com

* Corresponding author e-mail: yazdi_mt@yahoo.com

Late Cretaceous should not be considered as an indication of the collision of the Arabian plate with Iran.

In the Late Cretaceous, such a mixture was also formed in the south of Makran, while no intercontinental collision occurred in this region, and subduction continued. Some researchers believe that the continental collision between Arabia and Eurasia occurred during the Cenozoic era, for example, during the Eocene (Braud, 1987; Şengör et al., 1988, 1993; Ghasemi & Talbot, 2006), Eocene Oligocene (Berberian et al., 1982; Hooper et al., 1994), Oligocene time (Yilmaz, 1993; Agard et al., 2005), Oligo-Miocene time (Robertson et al., 1991; Golonka, 2004), Miocene time (Şengör & Kidd, 1979; Stoneley, 1981; Woodruff & Savin, 1989; Şengör & Natalin, 1996; Robertson, 2000; Axen et al., 2001; McQuarrie et al., 2003; Mohajjel et al., 2003; Guest, 2004; Homke et al., 2004; Allen et al., 2004) Pliocene time, (Philip et al., 1989) and Pliocene-Pleistocene time (Stocklin, 1977).

Also, according to Hassanzadeh et al., (2008), the magmatic belts of Alborz and Urmia-Dokhtar are both separated parts of the magmatic arc of the Neotethys unit. Carefully studying the tectonic developments of the Sanandaj-Sirjan zone, has attributed the different forms of the region to the operation of the northeast-southwest convergence regime of the Neotethys until the Cenozoic era (Tillman et al., 1981). Most of these different forms, which are folding and thrusting of the overlying sediments, are related to the operation of reverse and transfer faults during the convergence regime in the Late Cretaceous to Paleocene, which is the cause of the thrusting of Iran in the center of Sirjan and the folds within it is also plate and thrusting in Sanandaj-Sirjan zone (Tillman et al., 1981). The continuation of the convergence in the Cenozoic era has caused the subsidence of the pit along the northwest in the southwest of the reverse faults and the parallel uplift of the adjacent blocks in the northeast of the faults. The study of continental collision in the Sanandaj-Sirjan zone has considered the abduction of ophiolites in the northwest margin of the Arabian Plate as the result of the collision of the arc islands with the inactive Arabian margin in the Late Cretaceous, but they attributed the final continental collision between the Arabian Plate and Central Iran to the Miocene (Mohajjel et al., 2003). The geometrical pattern, propagation paths and their orientation, the thickness and spatial distribution of fudge dikes have a direct relationship with pre-existing faults of the type of stress regime during magma intrusion and the mechanical resistance of the host rocks because usually, the trend of dikes is parallel to the maximum horizontal compressive stress at the time of emplacement and perpendicular to the direction of tension (Pollard, 1987). Based on the geometrical pattern, Fudge dikes are classified into three general categories: parallel, small radial, and large radial (Hou, 2012). Each of these patterns shows the dominance of a type of tectonic pattern in the area. According to her, dikes are formed in parallel in regional stresses, but types with a small radial pattern of the Hole model (around volcanic and intrusive structures and huge radial types of Pre-Existing Hole) are observed in the fracture zones of large continents associated with the mantle plume. Swarms of mafic dikes are markers of thermal events in the upper mantle. In many cases, their formation is interpreted as a result of cracking and stretching of the craton's lithosphere, and they may characterize the initial stages of the formation of large igneous provinces above the mantle plumes (Ernst & Buchan, 1997; Ernst & Bleeker, 2010; Gladkochub et al., 2010). The dikes of the studied area are of small radial type.

The Iran plateau is a part of the Alpine–Himalayan orogenic belt generated by the opening and closure of the Tethys Ocean (Bagheri & Stampfli, 2008). Fudge dikes in Iran have been introduced and investigated in the Urmia Dokhtar zone, southeast of Shahrood and Biarjmand (Ghasemi et al., 2017), northwest of Zahedan (Sarhadi et al., 2016) and northern Mashhad Ardahal dikes (Hosseini et al., 2016). In the Bafq area, the floods of Rizo series (Nik Tabar & Rashidjademran, 2015), Narigan granite dikes (Mousavi Makui 1996), Chah Chole (Yazdi et al., 2013), and granitoid mafic dikes of Zarigan (TajBakhsh, 2019) have been mentioned and investigated, but so far no comprehensive study has been done about the intruded dikes around

southeast Bam. In this article, an attempt is made to investigate the lithology, geochemistry, genesis, and tectonomagmic environment of these dikes.

Geology

The studied area is located 120 km southeast of Bam city and between latitudes 28°03' to 28°24' north and longitudes 58°49' to 59°00' east. The mentioned area is located in the east of the Negisan sheet and south of the Jahanabad sheet.

Structurally, the studied area belongs to the tectonic range of central Iran (Dahij-Sardoye belt). One of these volcanic-intrusive chains is the Kerman Cenozoic Magmatic Assemblage or the Dehij-Sardoye belt (Dimitrijevic, 1973), which is currently located in the southern margin of the central Iranian subcontinent. The volcanic-sedimentary and volcanic-plutonic magmatic activity of this belt started from the Eocene and continued until the Quaternary. Significant magmatic events, accompanied by sedimentary processes, occurred during the Miocene. Most of Iran's porphyry copper mineralization has occurred on the Dahej-Sardoiyeh volcanic belt, which forms the southeastern part of the Urmia-Dokhtar zone. In this area, more than 50 traces of copper mineralization have been identified in the form of porphyry and veins along with elements of molybdenum, gold, silver, lead, zinc, etc.

The phenomenon of magmatism in this belt belongs to the Cenozoic era, which mainly acted as volcanism in the Eocene and as plutonism in the Oligo-Miocene (Abadian, 2010). In general, this batholith Jabal Barez is a multi-stage intrusive mass, where the three main phases of this mass are diorite, tonalite, and granite, respectively.

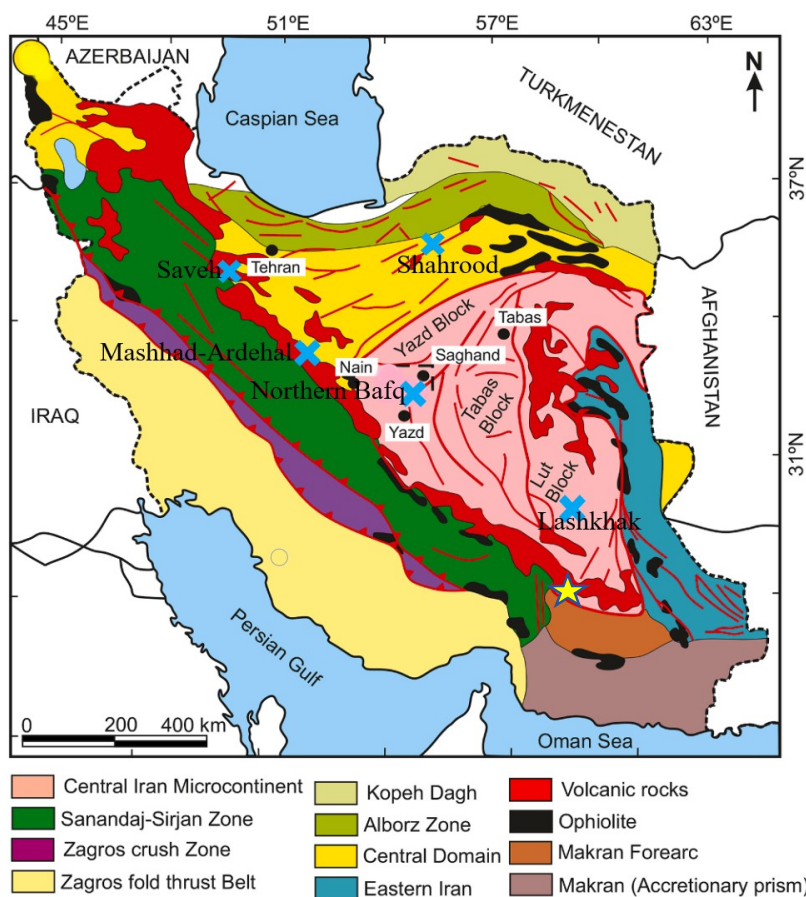


Figure 1. Simplified geological map of Iran. Regions are modified after Alavi (1991). The groups of dikes studied in Iran are marked with an asterisk

The Ngac unit (Mio-Pliocene) has a large expansion in the region and includes volcanic breccias and volcanic-sedimentary rocks, which are cut by numerous porphyry micro diorite dikes. In some areas, the thickness of this unit reaches 500 meters. This unit has a volcanoclastic origin and lithological studies in this unit indicate that the matrix of most of the rocks is of glass type. Lavas often have an andesitic composition. In the Negisan region, numerous dikes have been injected into different units. These dikes have different ages and most of them have been replaced by Eocene units. Most of these dikes have cut the batholith mass of Jabal Barez and even some dikes are connected with Quaternary volcanoes (Yazdi et al., 2019).

The oldest dikes in the area of Jabal Barez are dikes intruded in Eocene rocks, which may be the feeding network of volcanic rocks and Eocene igneous layers. In the context of the Jabal Barez intrusive body, especially granodiorites, there are very large dikes of dark-colored microdiorites with a northwest-southeast trend. Fine crystal dikes are cut by coarse crystal dikes, so they are older than them. Both types of dikes have rapidly cooled sides and their border with granodiorites is quite abrupt, which indicates that these dikes were injected after cooling and crystallization of the main intrusive body. In some areas, especially in the center of the intrusive bodies, both types of dikes contain xenoliths with the composition of hornblende-biotite diorites. In addition to the mentioned micro diorite dikes, some light-colored quartz feldspar dikes are also seen in the intrusive bodies of the area. The last intrusive member recorded in the Negisan area are alkaline dikes that have a limited extension. In terms of origin, these alkaline dikes are related to the Quaternary volcanic lavas of the area. In the southeastern region of Bam and Jabal Barez, three groups of dikes can be identified, which are micro-diorite dikes, micro-monzo-granite dikes, and andesite-basalt dikes (Al Taha, 2003).

Microdiorite dikes: Microdiorite dikes can be seen in intrusive rocks and Eocene volcanic. But in the west of the range and inside the granite unit, they have a significant expansion and density. It is difficult to distinguish these dikes from basaltic dikes (b) on aerial photographs, and the only difference between these two groups of dikes is the lighter color of micro diorite dikes (dark gray to brown) than basalt dikes (black). Meanwhile, the intensity of alteration in microdiorite dikes is usually higher.

Micro-granite dikes: only a few outcrops of dike-like micro-monzonite and micro-granite rocks are observed in the southeast and east of the study mass. These dikes, are very similar to the monzonite quartz intrusive body in terms of chemical and mineralogical composition and are most likely parts of the same main mass that merges with the monzonite quartz body at depth. These rocks are light gray in the hand sample. The texture of these rocks is partially porphyritic-granular, porphyries include corroded plagioclase (albite-oligoclase) and alkali feldspar.

C- Basaltic andesite dikes, these dikes along with andesite dikes are the most widespread in the studied area. These dikes with a length of about several meters and a thickness of several meters, along the NW-SE direction (in line with the main faults of the region) have usually been observed in different places. These dikes are easily distinguishable from their host rocks due to their color difference. These rocks are black in hand samples and fine grain background consisting of pyroxene and plagioclase and white feldspar phenocrysts.

Analysis methods

During field operations, 80 samples were taken in systematic sampling, of which 55 thin sections were prepared. The samples were among the fresh outcrops and the weathered rims of the samples were removed before packing in plastic sample bags. and were studied by using a Zeiss polarizing microscope at the Islamic Azad University, Science and Research Branch, Tehran.

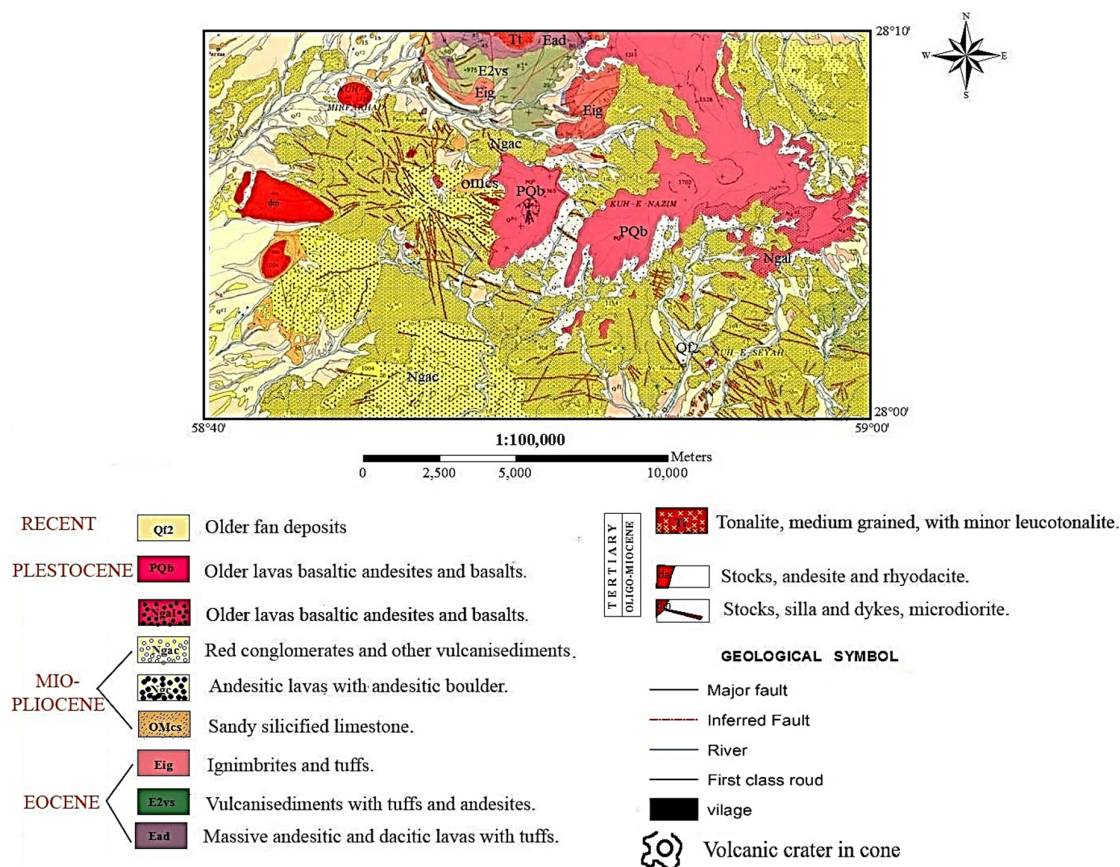


Figure 2. Geological map of the area (Eftekharnjad, 1989)

We used two main analytical procedures including: 1) X-Ray Fluorescence (XRF) and Inductively Coupled Plasma-Mass Spectrometry (ICP-MS) for whole-rock, major- and trace-element analyses; the samples analyzed in Zarazma Company of Iran.

Petrography

Andesite

They appear in macroscopic scale or hand samples in gray to grayish pink colors. Under the microscope, this rock consists of plagioclase and pyroxene phenocrysts embedded in a microcrystalline matrix. They have porphyritic and glomeroporphyritic textures. Plagioclase minerals are seen in anhedral, subhedral, and euhedral forms and indicate polysynthetic twinning and even zoning structures. The extinction angle measurements (An_{48-50}) show that they are of andesine type. Plagioclases make up 35 to 40% of the rock in thin sections. Pyroxene (diopside) crystals appear orange to pink under the polarized light. They are often subhedral and fine to medium crystals. These minerals make up about 10% of the rock in the thin section. Opaques are accessory minerals of this rock, making up 10% of the rock in thin sections. The secondary minerals of epidote, calcite, sericite, chlorite, and iron oxides are generated due to the alteration of plagioclase and pyroxene (Fig 3. A). The Opacitic rim or reaction rim is observed in the margin of some amphibole minerals. Opacitic rim or reaction rim is a common structure of hydrated mineral in volcanic rocks such as biotite or amphiboles. The amphiboles, during magma ascent, will decompose in response to the decrease in water pressures in the melt during ascent. Usually, the reaction rims on amphiboles consist of a complex assemblage of

minerals like clinopyroxene, plagioclase, magnetite, and ilmenite. The process of opacitic rim formations can be described as a devolatilization process. The amphiboles or biotite crystals release their structurally bound water to the magma in response to the decrease in water pressure in the magma as it ascends to the surface (Shelley, 1993; Vernon & Clarke, 2008).

Olivine basalts, Basalts

These rocks show porphyritic textures with microlithic to the vitreous matrix, however, glumero-porphyritic and amygdaloidal textures are sometimes observed (Fig. 3. F). The rock-forming minerals are plagioclase, clinopyroxene, and olivine, which are hosted by a matrix of plagioclase, clinopyroxene (augite), olivine, and opaque minerals or glass. Opaque minerals are accessory minerals while iddingsite (or bulangite), epidote, serpentine, and chlorite form the main secondary minerals. Matrix is formed from glass, plagioclase microlites, opaque minerals, and secondary minerals.

Dacite

This rock appears as light gray in the hand sample. The microscope view of the mineral indicates plagioclase crystals in a glassy and microcrystalline matrix. The texture of the rock is porphyritic. Plagioclase is euhedral, subhedral, and anhedral and makes up 30 to 35% of the rock matrix. These feldspars are oligoclase (in the Michel-Levy method). The alteration process converts them to calcite, chlorite, quartz, and iron oxides, making the minerals' surface cloudy. Quartz is found in small amounts and often as microcrystals in the rock matrix. The secondary minerals of these rocks are iron oxides, including hematite, magnetite, and limonite. Calcite, chlorite, sericite, iron oxides, and remnants of amphibole and biotite are visible in the rock. Iron oxides appear as inclusions inside the plagioclase crystals (Fig 3. c).

Gabbro-Diorite

Gabbro-dioritic rocks are coarse-grained and dark grey in color. They exhibit ophitic, granular, and microgranular texture (Fig. 3d, e) and minerals including 45–50% plagioclase with euhedral-subhedral shapes, 15–20% brown hornblende with euhedral-subhedral shapes, and 25–37% pyroxene (augite). Plagioclases are labradorite type and have low alteration. Accessory minerals are zircon and opaque minerals. The suite of secondary minerals includes biotite, sericite, calcite, iron oxides, and chlorite. Average grain size is about 0.5–4mm. the quartz content is less than 10% and the space between plagioclase fills the coarse crystal minerals. Reddish brown biotite, pleochroic crystals up to 1–2 mm can be seen from subhedral to non-hedral in size and form. The prevalence of high partial pressure of H₂O during crystal fractionation indicates hornblende (secondary) replacing pyroxene (Azer et al., 2012).

Granodiorites

These rocks are gray or greenish in color. They show granular and poikilitic textures. The main minerals in these rocks are plagioclase (~47%), quartz (~20%), K-feldspar (15–20%), and biotite (5–10%). Accessory minerals are chlorite, biotite, sericite, sphene, and clay minerals.

Plagioclase is the most prominent mineral of granodiorites and the type is andesine to labradorite. Some plagioclases have been decomposed into sericite. Quartz is subhedral with medium grain size filling the spaces between grains. Potassium feldspar of orthoclase type and some of its crystals decompose into clay minerals and sericite. Amphibole is the most abundant mafic mineral found in granodiorite with euhedral-subhedral shapes.

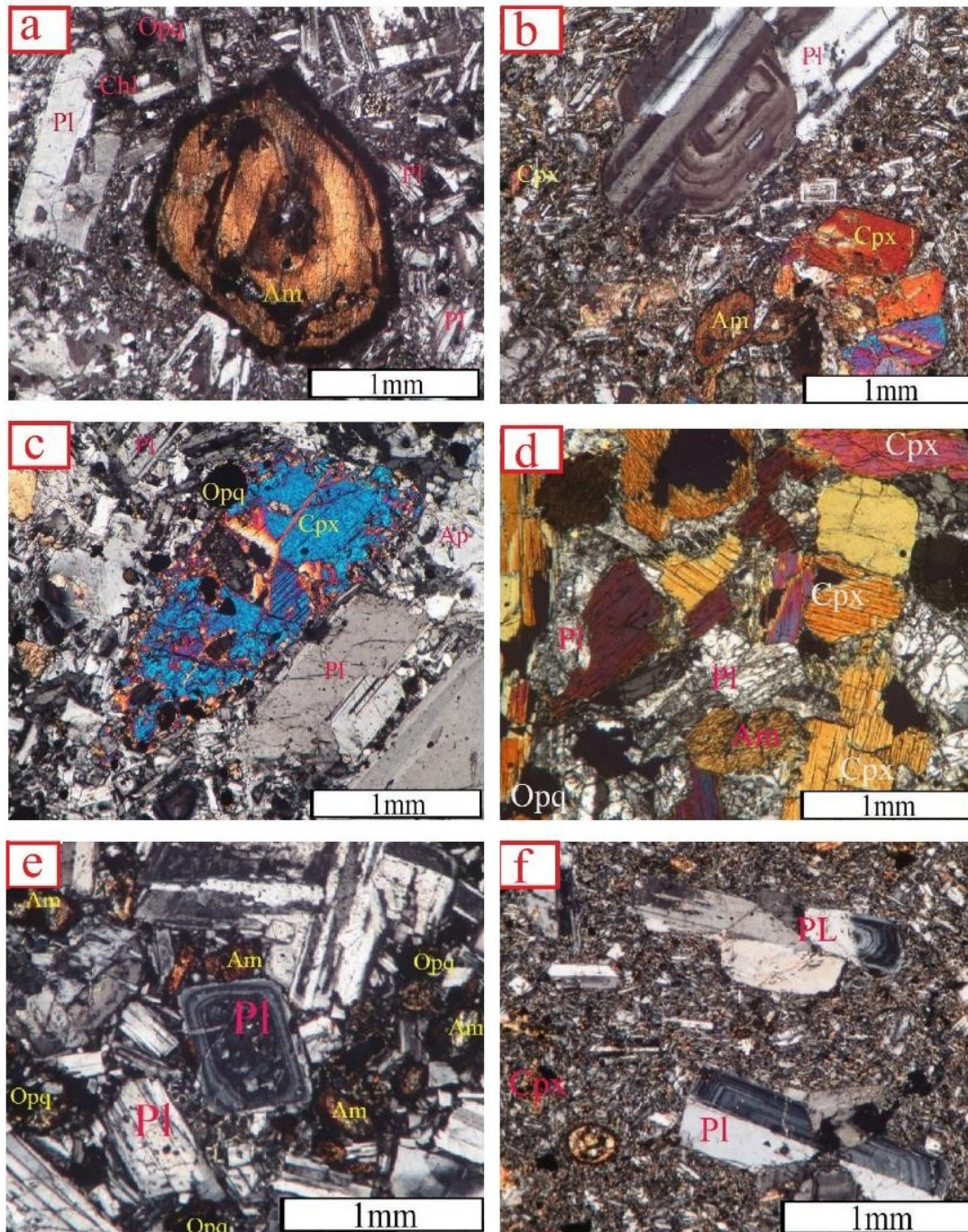


Figure 3. a-photomicrographs of (in cross-polarized light) showing porphyritic texture and opacified amphibole phenocryst and plagioclase in andesite. b- A view of the presence of plagioclase with fluctuating zoning, amphibole, and pyroxene in the diorite. c- A view of the granular texture with the presence of apatite, plagioclase, and pyroxene minerals. d-view of ophitic and granular texture in gabbro. e- A view of the granular texture with the presence of opacified plagioclase and amphibole minerals in the hornblende diorite. f- View of porphyritic texture in basalt

Geochemistry

magmatic processes, including fractional crystallization, magma mixing, contamination, or a mixture of these processes, can be identified by geochemical studies on the distribution of

different elements in the rock units of each region. The association between these elements is one of the most important aspects considered in geochemical studies. Using these relationships allows understanding of the environments and processes effective in rock evolution (Tables 1 and 2).

In the diagram of Cox et al., (1979) based on the weight percentage changes of $\text{SiO}_2\text{-K}_2\text{O}+\text{Na}_2\text{O}$, the dikes are mainly in the range of gabbro-diorite to gabbro and granodiorite (Figure 7a). Dikes under study plot in the sub-alkaline and metaluminum fields (Figure 7 b and p). This classification is completely consistent with the type of minerals found in these rocks. The major elements and characteristics of the dikes are investigated in the Harker diagrams (Figure 5).

In gabbros, with the increase in the amount of SiO_2 , the amount of K_2O and MnO shows an increasing trend and CaO shows a decreasing trend. In these samples, Na_2O and K_2O have positive compatibility and MnO , MgO , CaO , Fe_2O_3 , and TiO_2 have negative compatibility with SiO_2 . The trends observed for these oxides are in accordance with the removal of clinopyroxene, amphibole, and plagioclase in diorites, as documented by Gao and Zhou (2013). In gabbros and diorites, Al_2O_3 shows an increasing trend with a gentle slope.

The geochemical investigation of the main and minor elements in the composition of the bodies of the region does not indicate the fundamental differences between the gabbroic and diorite masses found in this area. In such a way that in the graphs of binary changes, these masses do not show two different trends from each other. It seems that these two bodies have the same origin. Probably, the reason for the compositional break in the chemical evolutionary processes is the result of different origins in the magmas producing the samples, or it depends on the type of magmatic transformation processes.

(Dufek & Bachmann, 2010) showed that the absence of intermediate compounds, which is called the Daly gap, is common, and they explain this phenomenon by the separation of crystals and liquids during the event of the intermediate stages of crystal separation, after which, in the complex Bimodal volcanisms that depend on crystal segregation do not produce magmas of intermediate composition.

Table 1. Representative whole rock analysis of the Miocene dikes (major elements in wt.%)

	SiO_2	Al_2O_3	BaO	CaO	Fe_2O_3	K_2O	MgO	MnO	Na_2O	P_2O_5	SO_3	TiO_2	LOI
A-2	69.56	15.3	0.11	3.48	2.55	1.82	0.83	0.1	4.69	0.09	0	0.24	1.27
A-5	67.3	15.05	0.11	5.04	3.38	1.83	0.79	0.06	4.36	0.05	0	0.3	1.84
A-7	60.72	16.87	0.11	5.81	5.27	1.59	2.61	0.08	4.23	0.09	0	0.58	2.07
A-8	75.66	12.04	0.11	2.65	2.72	2.09	0.16	0.05	3.56	0	0.15	0.3	0.62
A-11	59.62	17.48	0.11	6.95	5.9	1.19	3.44	0.11	3.95	0.07	0.06	0.59	0.54
A-15	58.31	16.43	0.11	6.71	5.83	1.3	3.18	0.07	4.01	0	0	0.65	3.43
A-17	56.65	16.22	0.11	6.2	5.99	1.44	3.44	0.11	4.08	0.08	0	0.66	2.06
A-20	61.14	16.59	0.11	5.1	6.54	1.7	1.07	0.15	3.86	0.06	0	0.57	3.02
A-22	54.58	17.49	0.07	8.49	7.16	1	4.36	0.12	3.43	0	0.5	0.71	1.80
A-26	56.58	16.52	0.07	4.78	5.7	1.46	2.61	0.13	4.7	0.08	0.07	0.53	2.61
A-29	54.69	18.09	0.07	7.27	6.54	1.09	4.06	0.11	4.34	0.06	0.08	0.67	2.83
A-35	52.34	16.46	0.07	8.61	7.48	0.91	5.6	0.13	2.96	0.06	0.05	0.78	2.52
A-36	57.47	17.15	0.07	7.06	6.92	1.03	3.73	0.11	3.94	0.18	0.13	0.62	1.58
A-38	69.27	15.3	0.07	3.54	2.61	1.84	0.82	0.13	4.83	0.05	0.05	0.24	1.26
A-39	60.33	18.03	0.07	6.5	5	1.34	2.07	0.08	4.34	0.06	0.18	0.58	1.40
A-40	60.34	16.65	0.07	6.44	5.78	1.22	3.22	0.1	3.85	0.12	0.05	0.55	1.59
A-41	59.23	17.53	0.07	6.41	5.98	1.29	3.13	0.11	4.33	0.06	0.05	0.57	1.28
A-45	66.22	14.3	0.07	4.42	4.17	2.33	1.57	0.09	4.1	0.06	0.12	0.45	2.09
A-46	56.31	16.58	0.07	5.42	6.26	1.27	3.76	0.1	4.59	0.2	0.35	0.57	2.52
A-47	58.67	17	0.07	6.73	6.08	1.2	3.4	0.11	4.26	0.16	0.23	0.57	1.48

Table 2. Representative whole rock analysis of the Miocene dikes (trace and rare earth elements in ppm)

	A-2	A-5	A7	A-8	A11	A15	A17	A20	A22	A-26	A-29	A-35	A-36	A-38	A-39	A-40	A-41	A-45	A-46	A-47
As	0.9	1.1	0.6	1	0.5	0.5	0.5	3.2	3.5	2.9	5.7	0.5	1.9	0.5	0.5	0.8	0.5	2.2	7.4	0.6
Ba	412	333	328	364	285	288	390	1259	753	322	256	243	272	386	335	274	281	385	268	298
Be	1.4	1.1	1.1	1	1	0.9	0.9	1.1	0.8	1	0.8	0.8	0.9	1.3	1	0.9	0.9	1.1	0.8	0.9
Bi	0.1	0.1	0.1	0.1	0.1	0.1	0.1	0.1	1.3	2.4	1	0.1	0.1	0.1	0.1	0.1	0.1	0.1	0.1	0.1
Cd	1.1	1.6	0.8	1.1	0.5	0.1	0.1	0.2	13.9	19.8	13	0.5	0.5	0.5	0.1	0.1	0.1	0.1	0.1	0.1
Ce	22	20	21	32	26	22	21	24	19	22	18	20	21	24	24	22	24	23	17	24
Co	2.8	6.9	13	2.2	17.1	15.5	15.9	9.6	20.4	12.7	18.6	24.1	18.3	2.9	11.3	15.3	14.6	8.9	14.5	15.5
Cr	4	11	34	6	55	47	51	25	62	19	64	81	32	2	28	47	37	15	19	45
Cs	1.7	1.3	0.8	0.5	0.7	0.6	0.5	0.7	1	0.5	0.5	0.5	0.5	2.2	0.6	1.1	0.5	0.6	1.9	0.7
Cu	4	19	38	28	63	55	54	51	58	44	58	45	52	2	48	49	42	23	40	40
Dy	0.9	1	1.5	1.7	2	1.9	1.6	1.9	2.1	1.6	1.8	2.4	1.9	0.9	1.7	1.8	1.8	1.4	1.5	1.8
Er	0.6	0.8	1	1	1.3	1.2	1.1	1.3	1.3	1.1	1.2	1.6	1.2	0.7	1.2	1.2	1.2	1	1.1	1.2
Eu	0.56	0.42	0.7	0.66	0.82	0.78	0.71	0.9	0.87	0.61	0.75	0.92	0.73	0.5	0.72	0.73	0.7	0.54	0.62	0.79
Gd	1.84	1.75	2.3	2.63	2.72	2.58	2.27	2.49	2.68	2.24	2.44	3	2.52	1.82	2.45	2.53	2.43	2.05	2.15	2.44
Hf	0.6	0.8	2.3	2	2.1	2.4	2.1	2.9	2	2	2	2.1	0.5	0.5	2.5	1.2	1.5	2.7	1.6	1.7
La	13	11	12	16	14	13	12	13	12	12	12	13	13	12	13	13	13	12	10	14
Li	31	22	21	28	21	19	19	18	8	18	15	7	12	25	20	19	18	21	26	16
Lu	0.1	0.1	0.1	0.2	0.2	0.2	0.1	0.2	0.2	0.2	0.2	0.2	0.2	0.1	0.2	0.2	0.2	0.2	0.2	0.2
Mo	0.9	1.1	0.6	1.3	0.7	0.6	0.5	0.5	0.5	0.8	0.8	1.1	0.8	0.6	1	0.9	0.5	0.6	1	0.6
Nb	6.2	4	5.7	3.9	6.2	4.3	3.8	3.5	4.1	3.6	3.2	4.2	3.3	3.6	3.9	4	3.3	3.4	3	3.7
Nd	9.3	6.6	9.5	12.3	10.9	11.2	9.8	10.3	9.9	9.4	10	12.5	10.1	7.7	10.8	10	10.1	8.7	8.1	10.6
Ni	2	6	15	4	26	19	19	10	26	8	29	54	15	<1	13	23	18	7	15	22
Pb	16	13	9	14	8	8	33	233	1059	1459	891	39	46	45	21	11	12	12	6	9
Pr	3.24	2.59	3.2	4.06	3.6	3.6	3.25	3.47	3.26	3.22	3.24	3.6	3.3	2.99	3.45	3.34	3.38	3.1	2.74	3.39
Rb	36	25	18	51	15	22	17	21	13	19	16	3	17	36	22	10	17	29	24	15
S	50	50	50	349	336	243	94	270	1868	156	171	50	50	50	654	91	50	50	441	303
Sb	0.5	0.5	0.5	0.5	0.5	0.5	0.5	0.5	0.5	2.8	0.5	0.5	0.5	0.5	0.5	0.5	0.5	0.5	0.5	0.5
Sc	2	3.5	9.3	2.6	14.1	13.2	11.1	10	17.2	7.7	15	21	15.4	1.7	8.3	11.7	10.3	6.4	9.5	12.8
Sm	2	1.6	2.2	2.6	2.6	2.7	2.4	2.8	2.7	2.2	2.4	3.1	2.5	1.8	2.6	2.5	2.4	2.1	2.2	2.7
Sn	3.6	0.1	2.5	0.1	0.4	3.1	0.1	0.1	8.1	15.4	6.4	0.1	0.1	0.1	0.1	0.2	0.1	0.1	0.1	0.1
Sr	481	292.8	581	306	640	651	591	627	1059	486.5	617.2	897.5	608.4	397.6	573.3	640.9	527.9	455.8	464.1	793.7
Ta	0.4	0.4	0.7	0.4	0.6	0.5	0.5	0.4	0.6	0.4	0.3	0.5	0.5	0.6	0.4	0.5	0.8	0.4	0.5	0.5
Th	2.6	2.2	2.3	3.2	2.1	2.1	1.8	2.7	1.8	1.7	1.6	1.8	2.1	2.2	2.2	1.6	1.7	2.4	1.4	1.8
Tl	0.1	0.1	0.1	0.1	0.1	0.1	0.1	0.1	0.1	0.2	0.1	0.1	0.1	0.1	0.1	0.1	0.1	0.1	0.1	0.1
Tm	0.1	0.1	0.1	0.1	0.1	0.1	0.1	0.2	0.2	0.1	0.1	0.2	0.1	0.1	0.1	0.2	0.1	0.1	0.1	0.1
U	0.4	0.3	0.6	0.9	0.5	0.6	0.5	0.8	0.5	0.4	0.5	0.5	0.3	0.3	0.5	0.3	0.4	0.7	0.5	0.5
V	16	42	97	9	111	120	126	103	160	106	149	170	143	16	89	100	101	67	107	109
Y	5.1	6.4	7.5	9.2	10.9	9.4	7.9	9.4	11.1	8.5	9.6	12.2	10.4	4.7	9.3	9.1	9.6	7.6	8.4	10.3
Yb	0.43	0.68	1	0.82	1.35	1.19	1.12	1.35	1.49	1.18	1.32	1.63	1.31	0.39	1.09	1.16	1.21	0.96	1.09	1.29
Zn	72	49	73	30	74	71	70	71	326	487	306	88	92	45	62	72	87	65	83	81
Zr	12	20	85	66	75	88	74	111	73	74	72	77	8	5	92	36	56	111	62	60

According to some other researchers (e.g., Christiansen and McCurry, 2008; McCurry et al., 2008), some A-type rhyolites are formed during intense crystal segregation events and from basaltic magmas separated from the mantle in the continental crust. In this case, crustal density like a filter suppresses magmas with intermediate composition. Therefore, sets with inherent bimodal characteristics appear along with A-type rhyolites; It should be mentioned that this density filtration is activated when the intermediate magmas are rich in iron and denser than the mafic and felsic magmas in the system (Christiansen & McCurry, 2008; McCurry et al., 2008). According to the field and geochemical studies, it seems that crustal assimilation and melting played a role in the formation of granitic magma. However, these possibilities do not exclude the role of immiscibility in creating the Daly gap (Daly, 1914).

The chondrite-normalized spider diagram of dikes supports fractional crystallization (FC) (Fig. 7). The pattern of the diagram results from a high amount of olivine, which is an insensitive mafic mineral associated with REE fractionation. REE and trace element distribution patterns of alkaline samples (dike bodes) show positive anomaly trends in large-ion lithophile elements (LILEs), light and medium REEs (LREEs and MREEs), Nb, and Ta—

elements related to alkaline within plate magmatism and similar to enriched mantle rock (McDonough and Frey 1989). The most characteristic high-field strength elements (HFSE) of Gabbro–Diorite bodies, e.g. Nb, Ta, Zr, Y, Ti, and heavy REEs (HREEs), had lower normalized values compared to LILEs. Nb, Ta, and Ti show negative anomalies (Fig. 7). Additionally, samples were enriched in LILEs that behave as incompatible elements (Rb and K). These characteristics are related to subduction-related magma, including calc-alkaline volcanic arcs of continental active margins (Gill, 1981; Pearce 1983; Wilson, 1989; Walker et al., 2001) (Fig. 7). Based on the geochemical and petrographic evidence presented above, negative Ti anomalies are thought to be associated with oxide fractionation; negative P anomalies in the studied samples are attributed to apatite fractionation and enriched in Rb, Th, U, Ta, Nb, REE (except Eu), Hf and Zr which can partition into titanite, zircon, ferrichterite and aegirine (Linnen & Keppeler, 2002; Marks et al., 2004; Prowatke & Klemme, 2005). The absence of plagioclase crystal fractionation results in a high Sr content, along with a lack of Eu anomalies.

The dikes formed from different mafic-basic magma sources by differentiation and crystallization processes. Highly incompatible element ratios minimize the effects of differentiation and provide the characteristics of a mantle source. The origin of the difference is reflected by different correlations in this ratio (Rollinson, 1993). In the diagram proposed by Saunders et al., (1988), different trends may confirm distinct magma sources for Gabbro–Diorite dikes in the region (Fig. 8). There are two trends on the MgO versus Zr diagram of Wilson, (1989) (Fig. 9).

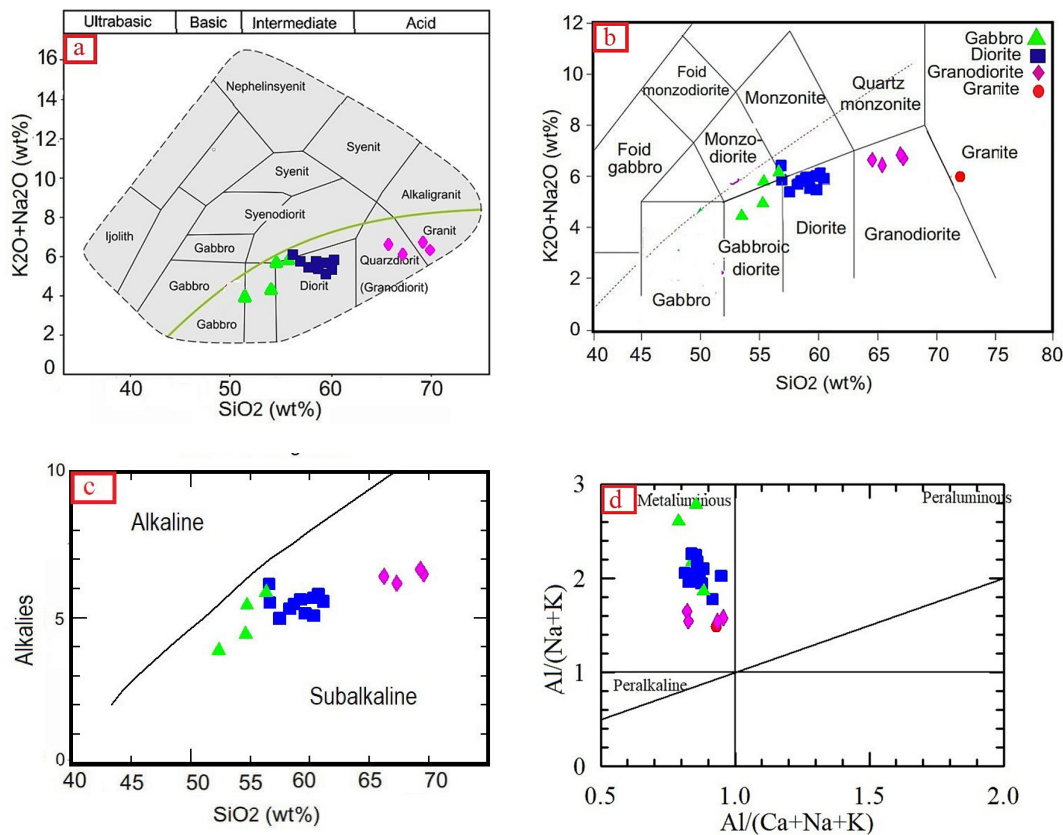


Figure 4. a) total alkalis (Na₂O + K₂O) vs. SiO₂ (TAS) diagram (Cox et al., 1979). b) total alkalis (Na₂O + K₂O) vs. SiO₂ (TAS) diagram (Irvine & Baragar, 1971). c) total alkalis (Na₂O + K₂O) vs. silica diagram (Middlemost, 1994). d) Plots of the samples in a [(Al₂O₃)/(Na₂O + K₂O)] vs [(Al₂O₃)/(Na₂O + K₂O + CaO)] discrimination diagram of (Maniar & Piccoli, 1989)

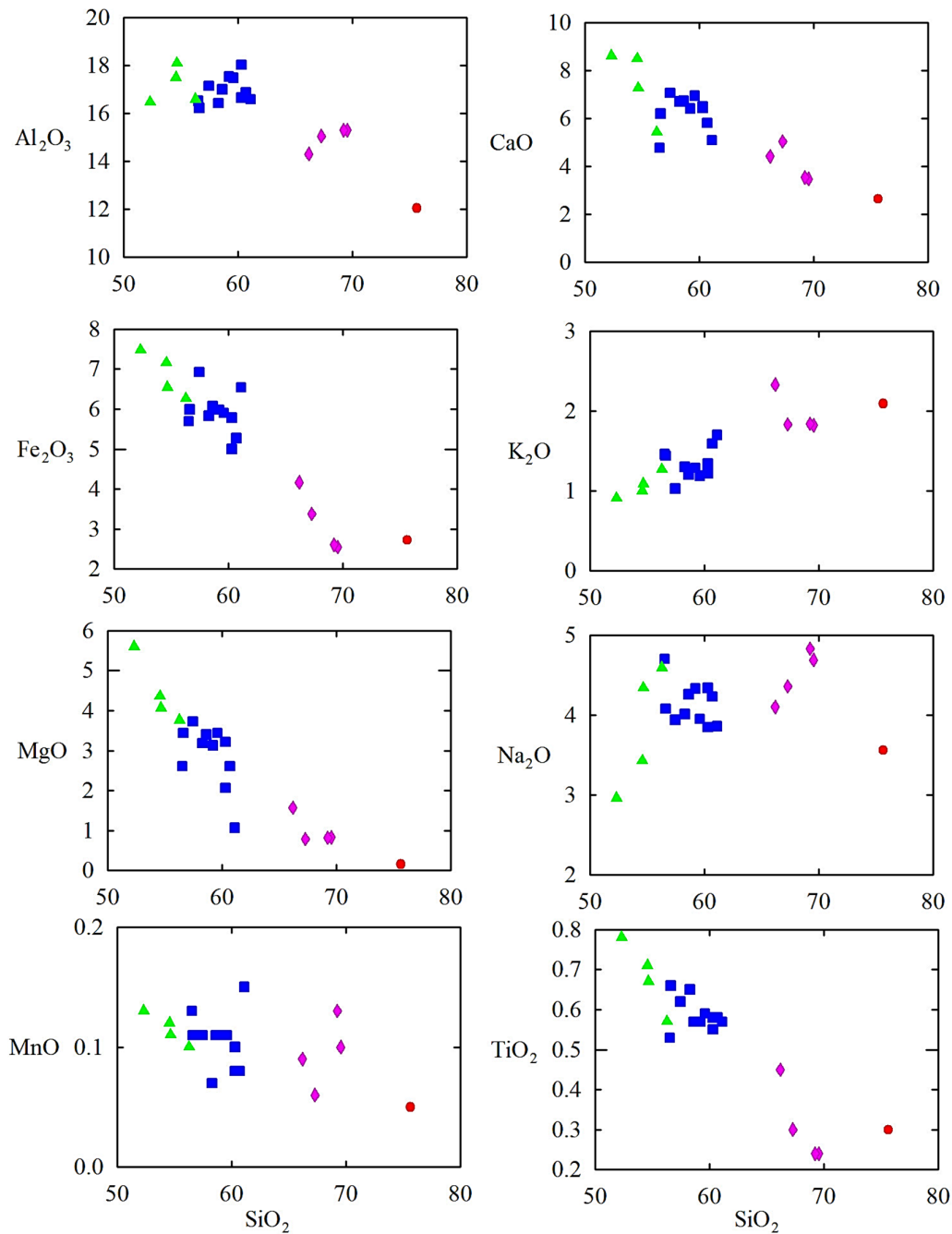


Figure 5. Harker diagrams for major oxides

The horizontal trend explains the different degrees of partial melting in the case of more than one magma source in the genesis of basic-mafic igneous rocks, consisting of different types of rocks, and the diagonal trend represents fractionation to form different rock types from a single basic-mafic magma source. In the light of field, mineralogical, and geochemical data, the MgO–Zr variogram of the rock types of the Gabbro–Diorite dikes can be considered to indicate a single mafic-basic magma source, and Gabbro–Diorite bodies can be considered to have formed from another single mafic-basic magma source (Fig. 9). It is crucial to note that Gabbro–Diorite dikes are alkaline and exhibit the geochemical characteristics of within-plate intrusion. These are different from other intrusions in the region with different tectono-magmatic characteristics and magma sources.

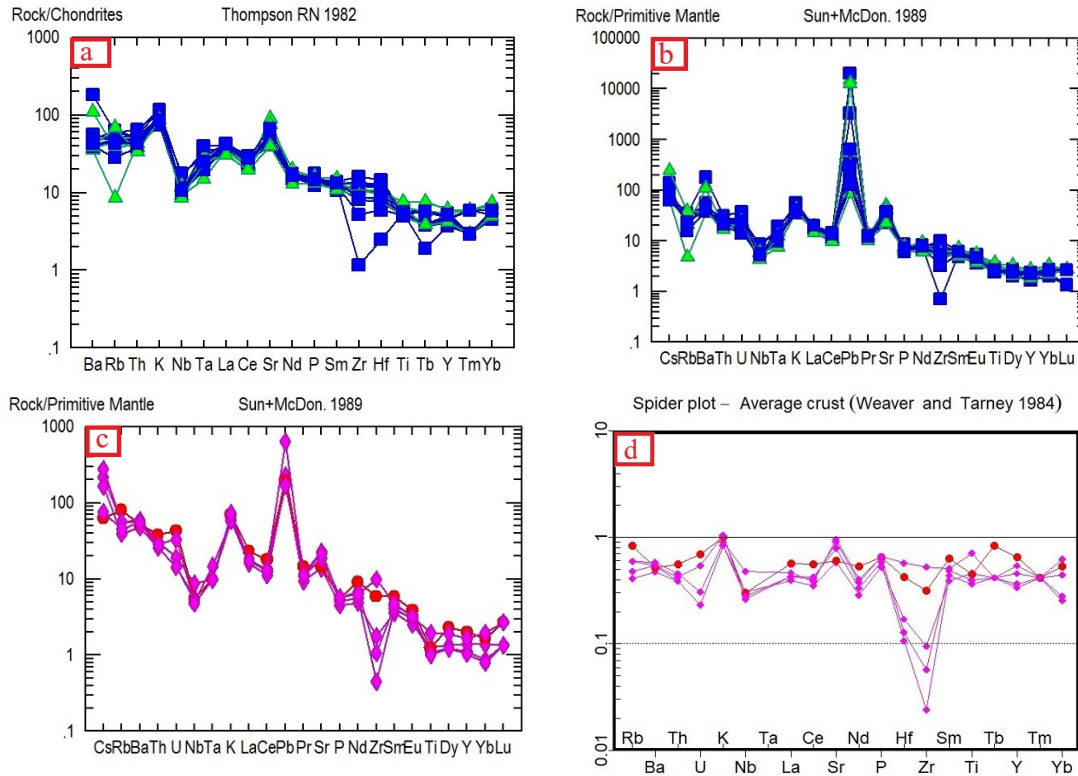


Figure 6. a-Rock/chondrite spider diagrams of the gabbro-diorite dikes (Thompson, 1982). b-rock/Primitive Mantle spider diagram of the gabbro-diorite dikes (Sun+McDon, 1989).c-Rock/chondrite spider diagrams of the Granodiorite dikes(Thompson, 1982). b- Average crust spider diagram of the Granodiorite dikes (Weaver & Tarney, 1984)

Partial melting of upper mantle material in such a geologic context is mainly generated by lithospheric attenuation under the tensional regime that created the immature rift that later closed (Harris et al., 1986; Wilson, 1989; Prichard et al., 1993). According to Bailey (1983), alkaline magmatic activity is generally controlled by the withdrawal of accumulated magma from volatiles originating from the mantle areas, and fractures in the continental lithosphere acting as magmatic channels. Volatile and incompatible elements in large mantle tanks escape through narrow fractures and rift zones. This results in metasomatism or melting a part and an expansion in mantle rock and the crust surrounding the tracts. In turn, the sills develop a within-plate character with an enriched mantle source. The emplacement of the Gabbro-Diorite dikes was contemporaneous with the development of the rift. The characteristics of gabbroic sills, including high K_2O/Na_2O , Fe/Mg , Zr , Nb , Y , and REEs, are consistent with an anorogenic origin (Loiselle, 1979).

A low Nb/Th ratio is one of the characteristics of continental crust (Rudnick & Fountain, 1995). This ratio is low in the studied samples of the region and varies from 1.25 to 2.95. In the diagram of Nb/Th vs. Th , all the samples are plotted in the field of lower continental crust (Figure 8). In this diagram, the diorite samples are placed in the average composition of the lower crust. However, the gabbro samples are located a little lower than the underlying continental crust. The Ce/Pb ratio is one of the other valuable characteristics to detect crustal pollution events because the continental crust has lower values of this ratio compared to the mantle. Also, processes such as partial melting and fractional crystallization have very little effect on this ratio (Hofmann et al., 1986). In the Ce/Pb versus Ce diagram, the samples are mostly located in the vicinity of the composition of the continental crust and confirm the presence of crust contamination in the studied samples (Figure 7-C). Also, in the diagram of K_2O/Na_2O against Rb/Zr , all the samples are along the AFC of fractional crystallization assimilation and contamination (Figure 7-D).

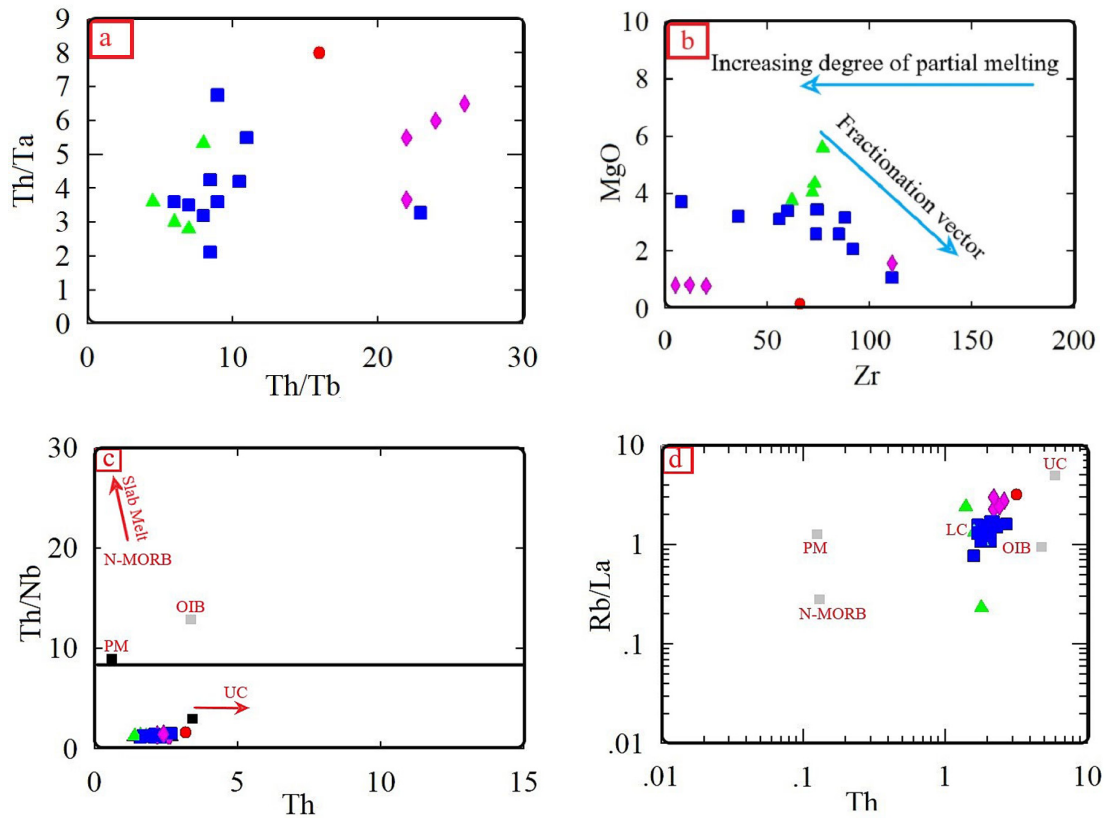


Figure 7. a- Incompatible element ratio diagram (Saunders et al., 1988). b- Trace and major element variograms of rock samples from Gabbro–Diorite bodies (Wilson, 1989). In diagrams c and d, the average composition of oceanic ridge basalts from Sun & McDonough, (1989), crust from Wedepohl, (1995), lower crust from Weaver & Tarney (1984), upper crust from McLennan, (1981) and others from Sun & McDonough, (1989)

Petrogenetic and geodynamic implications

To evaluate the tectonic setting of these intrusive bodies, the field, petrographic, and geochemical characteristics of these masses have been used. For this purpose, various tectonic environment discriminating diagrams have been used (figure 8). In some diagrams, magmatism features of arc islands and related to subduction, and in other diagrams, they are placed plotted within-plate. The granites exhibit similarities with volcanic-arc and within-plate granites in plots of Ta vs Yb (Figure 8. f). On the tectonic discrimination diagrams of Schandle & Groton (2002), the active continental margin field (Figure 8 e), respectively.

Examining the abundance of rare elements in these rocks, especially HFSE elements, shows that these elements have different concentrations in these two rock groups. The presence of different amounts of HFSE in mafic magmas coexisting with each other can be justified based on the degrees of partial melting in the source rock (Kamenetsky et al., 2001, Xu et al., 2000), melting at different depths or mantle origin (Deckart et al., 2005; Jourdan et al., 2007, or subtraction Aden & Frizz 1996), the proportions of incompatible elements in gabbros and diorites of the region do not have a very obvious difference from each other, for example, the Zr/Sm ratio in gabbros varies from 24 to 30 and in diorites from 2.76 to 40, and the Zr/Nb ratio in gabbros from 27.20 to 45.25 and in diorites from 13.8 to 29.18. In addition, the gabbro and diorite rocks of the region are characterized by LREE enrichment, high values of Sr, Al₂O₃, and Ba, low values of HREE(Y), and negative Nb anomaly with different intensities in gabbros and diorite.

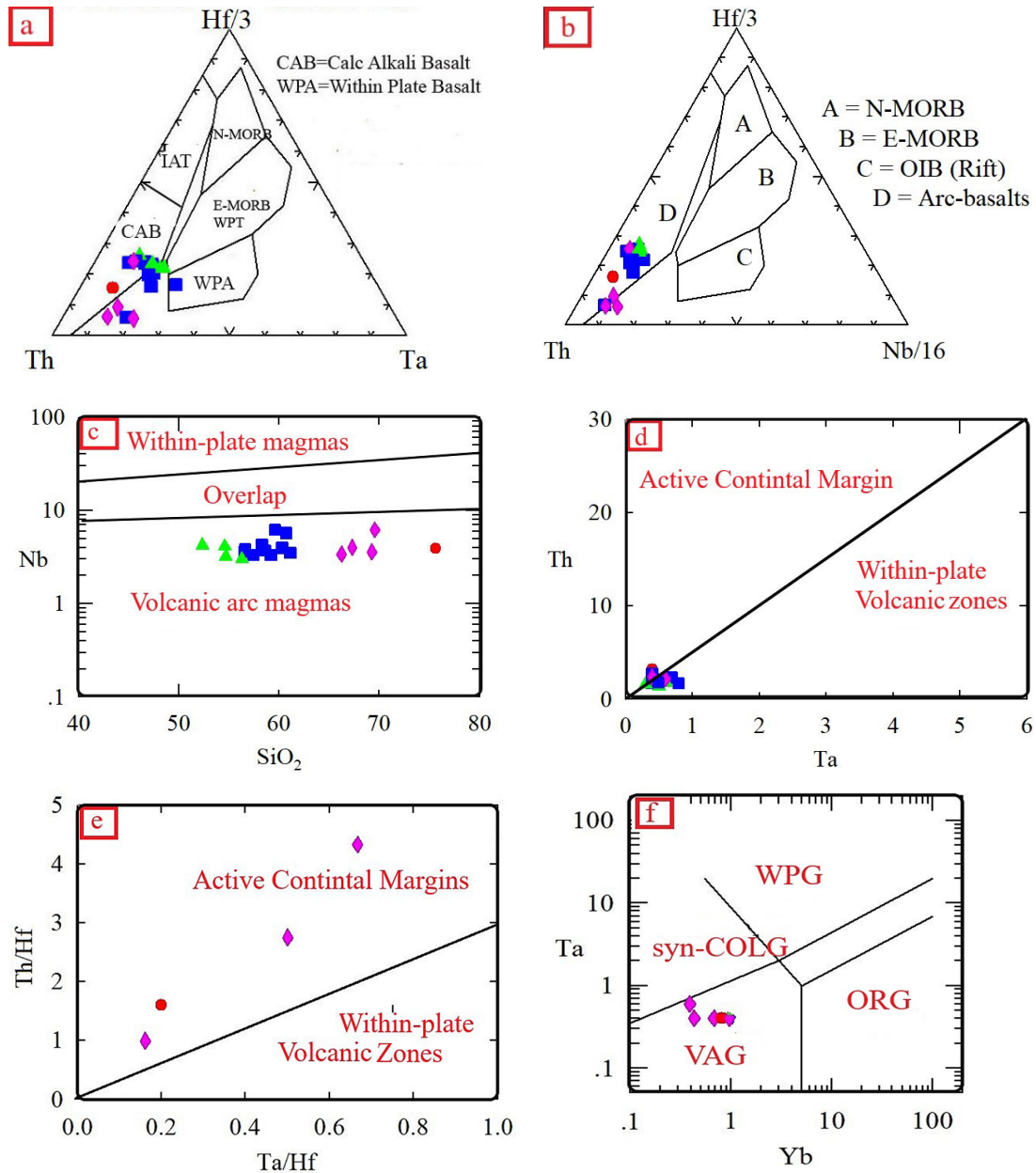


Figure 8. a-diagram for rocks in the Hf/3–Th–Ta diagram (Wood, 1980) b- diagram for rocks (Wood, 1980). c- diagram for rocks Pearce and Gale, 1977. d- Diagram of (Gorton & Schande, 2002). e- in the tectonic discriminant diagram (Schandle & Groton, 2002), all samples plot in an active continental margin field. f- Ta vs. Yb diagrams (Pearce et al., 1984)

The negative anomaly of Nb and low values of Nb/La ratio in these rocks indicate the contamination of the continental crust with primary magma during magma ascent or the involvement of crustal materials in the source area. In multi-element diagrams normalized to chondrite composition, the trends are more or less the same for gabbro and diorite rocks. Therefore, there is a possibility that these two rock groups are related to each other and formed from the same origin.

According to the geochemical relationships between various elements, differential crystallization is considered to be the main factor in changing the transformation of magmas that create the bodies of the region. Also, the presence of very small amounts of hydrous

minerals in gabbros and the significant increase in the amount of these minerals in diorite rocks (amphibole and biotite) as well as the increase in the amount of incompatible elements in the composition of these rocks indicate the presence of high amounts of fluids in the final stages of magma evolution (Fagan & Day, 1997; Stalder et al., 1998).

Also, magmatic contamination (AFC) has differentiated the geochemical composition of these two rock groups in the region (Fig 9. a-c). To investigate three important processes including fractional crystallization (FC), Mixing and absorption, and fractional crystallization (AFC) in the rocks of the region, we used different diagrams. In all three diagrams, the fractional crystallization process is dominant. In such a way that during the fractional crystallization of the gabbro body with the mineralogical composition of olivine, orthopyroxene, clinopyroxene, and plagioclase (rich in An) were formed in the first stages of magma cooling, while the later stages of cooling are accompanied by an increase in the concentration of volatile fluids and incompatible elements in the composition of the remaining magma, and at the end, the diorite body with the mineralogical composition of hornblende, biotite, and plagioclase (alkali) It is formed along with smaller amounts of clinopyroxene. This feature, along with the different distribution coefficient (Kd) of rare elements between the main minerals in the composition of gabbro and diorite, has caused obvious compositional differences between these two rock groups. In this regard, the separation of olivine, clinopyroxene, and magnetite in gabbros reduces the amount of MgO, Mn, TiO₂, and Fe₂O₃ elements in the remaining diorite magma. Abundant crystallization of biotite in diorite along with potassic alteration has caused the high level of potassium in diorite. The high Rb in diorite rocks compared to gabbroic rocks is due to the lack of a suitable place for this element in the structure of gabbro-forming minerals. The distribution coefficient of this element is high for phlogopite and sphene. The gabbros of the region do not have these minerals, and for this reason, this element is concentrated in the remaining magma and enters the biotite network in the diorite rocks in the next stages. Considering the fractional crystallization process and the concentration of plagioclase in gabbroic rocks, Sr in gabbroic rocks should have a high concentration compared to diorites, but geochemical investigations indicate relatively high amounts of Sr in diorites. The high abundance of Sr in diorite magma indicates the increase of this element due to crustal involvement (Rollinson, 1993). Nb element in diorite rocks has higher values than gabbroic rocks. The distribution coefficient of this element is relatively high for phlogopite and sphene minerals. The gabbros do not have these minerals. Therefore, due to the lack of a suitable place in the mineral network of gabbroic rocks, the Nb element is concentrated in the remaining magma and enters the biotite network in diorite rocks in the next stages. The concentration of Ce in diorite rocks is higher than that of gabbroic rocks. The distribution coefficient of this element in basaltic magma is less than one for most minerals. Therefore, during the subduction Taylor process, it is preferentially concentrated in the residual magma. The high Zr in diorite rocks compared to gabbroic rocks be explained by the distribution coefficient of this element in various minerals. The element Zr in the network of none of the main gabbro minerals, Kd for Zr in olivine, plagioclase, clinopyroxene, orthopyroxene, and magnetite is negligible. Therefore, it will be concentrated in the melt or diorite rock. Also, amphibole as one of the main minerals in diorite is considered a suitable host for this element. Kd for Zr in amphibole mineral is very high. The negative anomaly of Eu in diorite and the positive anomaly of Eu in gabbros is due to the high amounts of calcic plagioclase in gabbros (Rollinson, 1993). Similar conditions to those in the gabbroic and diorite intrusive masses of the region can be observed in Central Anatolia, Turkey (Buztug, 1998) and Khankandi intrusive masses located in Alborz (Agazadeh et al., 2010) and Nabi Jan region (Yazdani et al., 2016). According to various evidence, these researchers considered these intrusive masses to be the same origin. Examining the multi-element diagrams normalized to the primary mantle indicates the presence of negative HFSE anomaly, positive LILE anomaly

along with LREE enrichment, positive Pb anomaly, and negative Nb anomaly. These features are among the obvious features of calc-alkaline magmatism in the active continental margin (Sun & McDonough 1989), although in this case, other geochemical features of these rocks are distinct from active continental sites. Among these features, we can include relatively high amounts of Na_2O and relatively low amounts of K_2O in the composition of these rocks (the amount of Na_2O is always higher than K_2O). Relatively high values of Nb (up to 4.7 ppm in gabbros and 3.5-3.7 ppm in diorites) (Martin et al., 2005), absence of positive anomalies for Sr and negative for Ti, high Zr values of 77-62 ppm in gabbros and 112-75 ppm in diorites. Therefore, according to the results of the discriminating diagrams for the masses as well as the multi-element diagrams normalized to the primary mantle, it seems that these rocks are formed from an origin with hybrid and hybrid characteristics between the in-plane positions and the active continental margin. In this regard, the low Th/Ce ratio of 0.082-0.090 for gabbros and 0.10-0.070 for diorites in these samples indicates the metasomatism of the origin with fluids released from the sub ducting crust along with small amounts of melt-derived from the subducting crust or pelagic sediments. (Hawkesworth et al., 1997). Dilek et al., 2010 examined the rocks of the Caucasus of Azerbaijan with the Cenozoic PlioQuaternary age and compared the results with the Cenozoic rocks of North and North-West Iran and East Turkey. According to their research, all these rocks display a strong enrichment of Th, Ba, Rb, and La and a depletion of Y, Ti, and Yb compared to the composition of the primary mantle. They are mainly under the influence of FC and AFC processes. We used the diagram (Zhang et al., 2006; Imaoka et al., 2014) to calculate the amount of partial melting of different mantle sources.

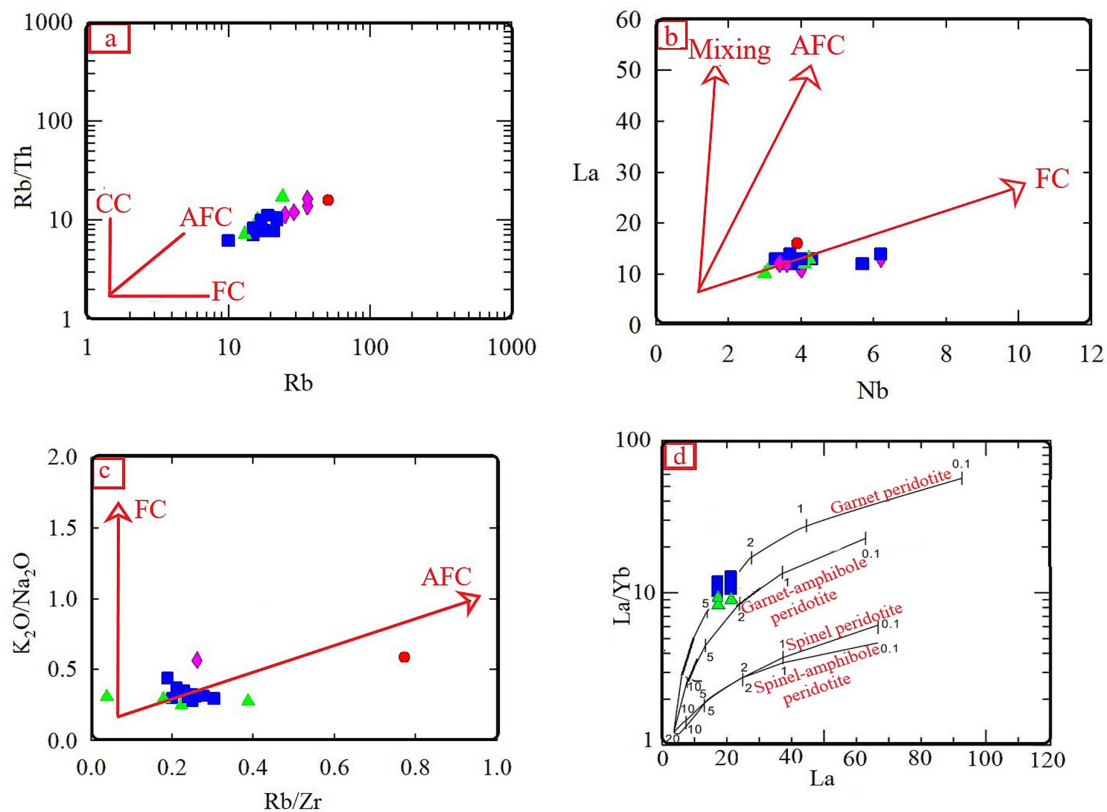


Figure 9. a-diagram for rocks of (Tchameni et al., 2006). b- La vs. Nb diagram, fractional crystallization (FC), assimilation-fractional crystallization (AFC), and mixing for rocks (Paulick et al., 2006). c- diagram for rocks of (Esperanca et al., 1992). d-Diagrams of (a) La vs. La/Yb, and (b) Nb vs. Yb, which model the partial melting of the different mantle sources (Imaoka et al., 2014; Zhang et al., 2006)

These rocks fall close to the garnet peridotite melting curves (Fig. 9.D) and are derived from a higher degree of partial melting of garnet peridotite (2-5%). The rocks have been attributed to the partial melting of the mantle lithosphere under the continental crust that has been placed under the influence of subduction (they have inherited the characteristics of previous subduction). These characteristics can lead to the formation of magma with hybrid and hybrid characteristics. Such characteristics are mainly seen in magmas related to the end of subduction and after impact (Chen et al., 2014, Yang et al., 2014). Any model presented for the tectonomagmatic setting of the region should be able to justify things such as the association of igneous rocks with Layers of tuffites and shallow marine sediments, the occurrence of magmatic activity after the end of subduction and continental collision or in the final stages of subduction, as well as the intermediate geochemical nature of these igneous rocks. The absolute age of the dikes under study is uncertain. Outside the studied area, the dikes in the north of Mashhad Ardahal have a lithological composition of basaltic andesite, andesite, and trachyandesite, which have penetrated into Eocene sedimentary and igneous rocks and represent part of the Tertiary magmatic activity in the middle part of the Urmia-Dakhter magmatic belt. These igneous rocks (Mashhad Ardahal dikes) with the characteristics of magmas in subduction zones show the geochemical characteristics of igneous rocks formed in arc islands and active continental margins, which were formed in a tensile basin behind the Ensialic back arc (Hosseini et al., 2015). According to Emami & Amini, (1375), these dikes have been introduced as feeding dikes of Tertiary volcanic units in the region. The andesite and basaltic andesite dikes located in the Miocene sedimentary units in the esker area in the Urmia-Dakhtar magmatic belt are also the result of subduction-related calc-alkaline magmatism, which indicates the dominance of the subduction-related regime of the Neotethys oceanic crust of the Arabian plate to the Central Iran plate in the active continental margin in the region (Chekni Moghadam et al., 2015). Of course, the primary magma of the volcanic rocks of the region probably originated from the melting of a part of the mantle, which itself is subsiding due to contact with flows derived from the oceanic crust and is enriched with rare elements. Geological studies have demonstrated that the geochemical characteristics of gabbro–diorite bodies are similar to those of subduction-related magmas attributed to the movements of CEIM (Central-East Iranian Micro-continent) relative to the Turan plate and/or the subduction of the Arabian Plate beneath CEIM. In the new model, subduction of the Arabian plate beneath CEIM—resulting in a primarily extensional regime and crustal thinning—caused the upwelling of the asthenosphere (Ramezani & Tucker 2003; Kargaran et al., 2006; Verdel et al., 2007; Kargaranbafghi et al., 2010, 2011).

Figure 10 shows a hypothetical tectonic model of dikes in the region. The geochemistry of the dikes indicates a source of subcontinental lithospheric mantle altered by subduction.

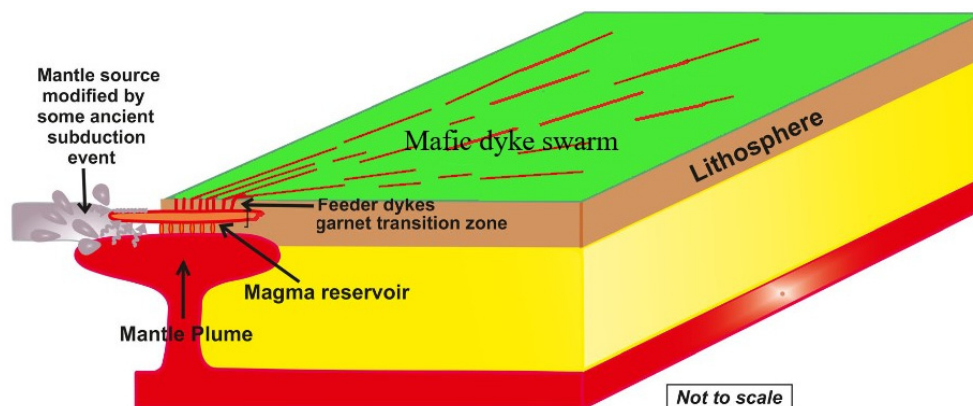


Figure 10. This picture shows a hypothetical tectonic model of dikes in the region (which has been adopted from the plan of Yadav & Sarma, 2020)

This magma reservoir, which must exist under moderate pressure, at a depth of 60 to 40 km, is thought to have been derived from the mantle plume. Magmatic intrusions through a series of fractures (feeder dikes), which spread across the region in the form of giant radiating dikes.

Conclusion

According to field, mineralogy, petrographic, geochemical, and petrological studies, the rock types include basalt, andesite, trachyandesite, dacite, and gabbro. The result of whole rock analysis indicates that reducing MgO content is accompanied by an increase in Al₂O₃, K₂O, Na₂O, and SiO₂ and a decrease in Fe₂O₃ and CaO concentrations. Therefore, these data confirm a metasomatic lithosphere mantle origin and the important role of fractional crystallization in the evolution of these rocks. The current tectonomagmatic regime is related to the continental collision environment where the main component is compression with a secondary tensile component due to right-strike slip faults. It seems that the tensile component in this part of the Urumieh-Dokhtar magmatic zone causes pressure reduction on the asthenospheric mantle and re-initiation of partial melting and magma rising to the surface. As a result, fractional crystallization and contaminations have occurred to some extent.

References

- Abedian, N., Barna, B., Saudi Shaar, P., Ali Akbari, H.A., 2010. preparation of economic geological map 1:25.000 of Ziaratshah-Komahi area located in 1:100.000 Negisan, Geological Organization, and mineral discoveries.
- Aden, A.J., Frizzo, P., 1996. Geochemistry and origin of low and high TiO₂ mafic rocks in the Barkasan complex: a comparison with common Neoproterozoic gabbros of northern Somali crystalline basement. *Journal of African Earth Sciences*, 22: 43-54.
- Agard, P., Omrani, J., Jolivet, L., Mouthereau, F., 2005. Convergence history across Zagros (Iran): Constraints from collisional and earlier deformation. *International Journal of Earth Sciences*, 94: 401-419.
- Aghazadeh, M., Castro, A., Badrzadeh, Z., Vogt, K., 2011. Post-collisional polycyclic plutonism from the Zagros hinterland: the Shaivar Dagh plutonic complex, Alborz belt, Iran. *Geological Magazine*, 148: 980-1008.
- Aghazadeh, M., Castro, A., Omran, N. R., Emami, M. H., Moinvaziri, H., Badrzadeh, Z., 2010. The gabbro (shoshonitic)-monzonite-granodiorite association of Khankandi pluton, Alborz Mountains, NW Iran. *Journal of Asian Earth Sciences*, 38: 199-219.
- Alavi, M., 1991. Sedimentary and structural characteristics of the Paleo-Tethys remnants in northeastern Iran. *Geological Society of America Bulletin*, 103: 983-992.
- Allen, M., Jackson, J., Walker, R., 2004, Late Cenozoic reorganization of the Arabia-Eurasia collision and the comparison of short-term and long-term deformation rates. *Tectonics*, 23(2). TC2008. doi:10.1029/2003TC001530.
- Al Taha, B., 1382. Petrography and petrology of igneous rocks and related mineralization in the southeast region of Bam Jabal Barez, Ph.D. thesis, Islamic Azad University, Science and Research Unit, Tehran, Iran. 290 p.
- Axen, G.J., Lam, P.J., Grove, M., Stockli, D.F., Hassanzadeh, J., 2001. Exhumation of the west-central Alborz Mountains, Iran, Caspian subsidence, and collision-related tectonics. *Geology*, 29: 559-562. doi: 10.1130/0091-7613(2001)029<0559:EOTWCA>2.0.CO;2.
- Azer, M. K., Abu El-Ela, F. F., Ren, M., 2012. The petrogenesis of late Neoproterozoic mafic dyke-like intrusion in south Sinai, Egypt. *Journal of Asian Earth Sciences*, 54-55(1): 91-109.
- Bailey, D.K., 1983. The chemical and thermal evolution of rifts. *Developments in Geotectonics*, 19: 585-597.
- Bagheri, S., Stampfli, G. M., 2008. The Anarak, Jandaq, and Posht-e-Badam metamorphic complexes in Central Iran: new geological data, relationships, and tectonic implications. *Tectonophysics*, 451:123-155.

- Berberian, F., Muir, I., Pankhurst, R., Berberian, M., 1982. Late Cretaceous and early Miocene Andean-type plutonic activity in northern Makran and Central Iran. *Journal of the Geological Society*, 139: 605-614.
- Boztug, D., 1998. Post-Collisional Central Anatolian Alkaline Plutonism, Turkey. *Turkish Journal of Earth Sciences*, 7: 145-165.
- Braud, J., 1987. La suture du Zagros au niveau de Kermanshah (Kurdistan iranien): reconstitution paleogeographique evolution geodynamique magmatique et structurale. PhD thesis, Universite Paris-Sud, 1-430p.
- Chekani Mogaddam, Sadeghian, M., Alimohammadian, H., 2012. The study of melt distribution in mafic dikes cutting the Delbar Biyarjomand metamorphic complex by means of the AMS method and determination of their paleopole position. Master's thesis, Shahrood University. 250p.
- Chen, Y., Zhu, D. C., Zhao, Z. D., Meng, F.-Y., Wang, Q., Santosh, M., Wang, L.Q., Dong, G.C., Mo, X.X., 2014. Slab breakoff triggered ca. 113 Ma magmatism around the Xainza area of the Lhasa Terrane, Tibet. *Gondwana Research*, 26: 449-463.
- Christiansen, E. H., McCurry, M., 2008. Contrasting origins of Cenozoic silicic volcanic rocks from the western Cordillera of the United States. *Bulletin of Volcanology*, 70: 251-267.
- Cox, K.G., Bell, J.D., Pankhurst, R.J., 1979. The interpretation of igneous rocks, Allen and Unwin, London, 450 P.
- Daly, R.A., 1914. *Igneous rocks and their origin*: New York, McGraw-Hill, 563 p.
- Dilek, Y., Imamverdiyev, N., Altunkaynak, S., 2010. Geochemistry and tectonics of Cenozoic volcanism in the Lesser Caucasus (Azerbaijan) and the peri-Arabian region: collision-induced mantle dynamics and its magmatic fingerprint. *Journal International Geology Review*, 52: 536-578.
- Dimitrijevic, M. D., 1973. Geology of Kerman region, Geology Survey of Iran. Report. Report Yu/52., PP 334.
- Dufek, J., Bachmann, O., 2010. Quantum magmatism; magmatic compositional gaps generated by melt-crystal dynamics. *Geology (Boulder)*, 38(8): 687-690.
- Eftekharnjad, J., 1989. Geological map 1:10000 of Negisan. Publications of Geological Organization of Iran.
- Emami, M.E., Amini, B., 1996. Geological map of Aran, scale 1/10000, Organization of Geology and Mineral Exploration of the country.
- Ernst, R.E., Bleeker, W., 2010. Large igneous provinces (LIPs), giant dyke swarms, and mantle plumes: significance for breakup events within Canada and adjacent regions from 2.5 Ga to the present. *Canadian Journal of Earth Sciences*, 47: 695-739.
- Ernst, R.E., Buchan K.L., 1997. Giant Radiating Dyke Swarms: Their Use in Identifying Pre-Mesozoic Large Igneous Provinces and Mantle Plumes Book Editor(s): John J. Mahoney, Millard F. Coffin. <https://doi.org/10.1029/GM100p0297>
- Ernst, R.E., 2014. *Large Igneous Provinces*. Cambridge University Press, Cambridge, 666.
- Ernst, R.E., Buchan, K.L., West, T.D, Palmer, H.C., 1996. Diabase (dolerite) dyke swarms of the world: first edition, Geological Survey of Canada Open File, 3241.
- Ernst, R.E., Head, J.W., Parfitt, E., Grosfils, E., Wilson, L., 1995. Giant radiating dyke swarms on Earth and Venus. *Earth Science Reviews* 39: 1-58. [https://doi.org/10.1016/0012-8252\(95\)00017-5](https://doi.org/10.1016/0012-8252(95)00017-5).
- Esperanca, S., Crisci, M., de Rosa, R., Mazzuli, R., 1992. The role of the crust in the magmatic evolution of the island Lipari (Aeolian Islands. Italy). *Contributions to Mineralogy and Petrology*, 112: 450-462.
- Fagan, T.J., Day, H.W., 1997. Formation of amphibole after clinopyroxene by dehydration reactions: Implications for pseudomorphic replacement and mass fluxes. *Geology* 25: 395-398.
- Fahrig, W.F., 1987. The tectonic settings of continental mafic dyke swarms: failed arm and early passive margin, In *Mafic Dyke Swarms* (eds) H C Halls and W F Fahrig Canada: Geological Association of Canada, 34: 331-348.
- Gao, Z., Zhang, H., Yang, H., Pan, F., Luo, B., Guo, L., Xu, W., Tao, L., Zhang, L., Wu, J., 2018. Back-arc basin development: constraints on geochronology and geochemistry of arc-like and OIB-like basalts in the Central Qilian block (Northwest China). *Lithos*, 310-311: 255-268. <https://doi.org/10.1016/j.lithos.2018.04.002> .
- Ghasemi, A., Talbot, C.J., 2006. A new scenario for the Sanandaj- Sirjan zone (Iran). *Journal of Asian Earth Sciences*, 26: 683-693.

- Ghasemi, H., Rostami Hasori, M., Sadeghian, M., 2017. Basic magmatism in the Lower-Middle Jurassic back-arc extensional basin in the northern edge of the central Iran zones south of Alborz-Sharghi, Shahrood-Damghan. *Earth Science Quarterly*, 27(107): 123-136.
- Gill, J.B., 1981. *Orogenic andesites and plate tectonics*, 390. Springer, Berlin.
- Gladkochub, D.P., Donskaya, T.V., Wingate, M.T.D., Mazukabzov, A.M., Pisarevsky, S.A., Sklyarov, E.V., Stanevich, A.M., 2010. A one-billion-year gap in the Precambrian history of the southern Siberian Craton and the problem of the Transproterozoic supercontinent: *American Journal of Science*, 310: 812-825. doi:10.2475/09.2010.03.
- Goldberg, K., Humayun, M., 2010. The Applicability of the Chemical Index of Alteration as a Paleoclimatic Indicator: An Example from the Permian of the Parana Basin, Brazil. *Paleogeography, Palaeoclimatology, Palaeoecology*, 293: 175-183 .
- Golonka, J., 2004. Plate tectonic evolution of the southern margin of Eurasia in the Mesozoic and Cenozoic. *Tectonophysics*, 381: 235-273.
- Guest, B., 2004. The thermal, sedimentological, and structural evolution of the central Alborz Mountains of northern Iran: Implications for the Arabia-Eurasia continent-continent collision and collisional processes in general [Ph D. thesis]: University of California, Los Angeles, 292p.
- Harker, A., 1909. *The natural history of igneous rocks*. Methuen and Company, London, 344p.
- Harris, N. B. W., Pearce, J. A., Tindle, A. G., 1986. Geochemical characteristics of collision zone magmatism. *Collision tectonics*, Geological Society of American Bulletin, 19: 67-81.
- Hassanzadeh, J., Axen, G., Guest, B., Stockli, D.F., Ghazi, A.M., 2004. The Alborz and NW Urumieh-Dokhtar magmatic belts, Iran: rifted parts of a single ancestral arc. Geological Society of America National Meeting. Geological Society of America, Denver, Colorado, 434.
- Hawkesworth, C.J., Turner, S., Peate, D., McDermott, F., Calsteren, P., 1997. Elemental U and Th variations in island arc rocks: implications for U-series isotopes. *Chemical Geology*, 139: 207-221.
- Hofmann, W. A., Jochum, K.P., Seufert, M., White, W. M., 1986. Nb and Pb in oceanic basalts: new constraints on mantle evolution. *Earth and Planetary Science Letters*, 79:33-45, [https://doi.org/10.1016/0012-821X\(86\)90038-5](https://doi.org/10.1016/0012-821X(86)90038-5)
- Homke, S., Verges, J., Garces, M., Emami, M., Karpuz, R., 2004. Magnetostratigraphy of Miocene-Pliocene Zagros foreland deposits in the front of the Push-e-Kush Arc (Lurestan Province, Iran). *Earth and Planetary Science Letters*, 225: 397-410.
- Hooper, R.J., Baron, I.R., Agah, S., Hatcher, R.D., 1994. The Cenomanian to the recent development of the Southern Tethyan Margin in Iran, in Al-Husseini, M.I., ed., *Middle East petroleum geosciences*. *Geology*, 505-516.
- Hosinie, H., Ahmadi, A.R., Ghanbari Dolatabadi, M., 2017. The origin and tectonomagmatic setting of dykes in the North of Mashhad-Ardehal. *Scientific Quarterly Journal*, 26: 187-198.
- Hosseini, B., Ahmadi, A., Ghanbari Dolatabadi, M., 2016. The origin and location of tectonomagmic dykes in the north of Mashhad, Ardahal, *Scientific-Research Quarterly of Earth Sciences*, 26(104): 198-187.
- Hosseini, S.Z., 2015. Geochemistry, petrogenesis, and tectonic environment of Eocene mafic lava flow in Sarcheshme, southwest of Rafsanjan. *Scientific-Research Quarterly of Earth Sciences*, 25(100): 209-220.
- Hou, G., 2012. Mechanism for three types of mafic dyke swarms. *Geoscience Frontiers*, 3(2): 217-223. <https://doi.org/10.1016/j.gsf.2011.10.003>.
- Imaoka, T., Nakashima, K., Kamei, A., Itaya, T., Ohira, T., Nagashima, M., Kono, N., Kiji, M., 2014. Episodic magmatism at 105 Ma in the Kinki district, SW Japan: petrogenesis of Nb-rich lamprophyres and adakites, and geodynamic implications. *Lithos*, 184-187, 105-131.
- Irvine, T.N., Baragar, W.R.A., 1971. A guide to the chemical classification of the common volcanic rocks. *Canadian journal of earth science*, 8: 523-276. <https://doi.org/10.1139/e71-055>.
- Jourdan, F., Bertrand, H., Schärer, U., Blichert Toft, J., Féraud, G., Kampunzu, A.B., 2007. Major and Trace Element and Sr, Nd, Hf, and Pb Isotope Compositions of the Karoo Large Igneous Province, Botswana-Zimbabwe: Lithosphere vs Mantle Plume Contribution. *Journal of Petrology*, 48(6): 1043-1077, <https://doi.org/10.1093/petrology/egm010>
- Kjøll, H.J., Galland, O., Labrousse, L., Andersen, T.B., 2019. Deep section of a Neoproterozoic fossil magma rich rifted margin exposed, EGU General Assembly 19: Vienna.
- Kamenetsky, V.S., Crawford, A.J., Meffre, S., 2001. Factors Controlling Chemistry of Magmatic

- Spinel: An Empirical Study of Associated Olivine, Cr-Spinel and Melt Inclusions from Primitive Rocks. *Journal of Petrology*, 42: 655-671.
- Kargaran, F., Neubauer, F., Genser, J., Houshmandzadeh, A., 2006. The Eocene Chapedony metamorphic core complex in Central Iran: preliminary structural results. *Geophysical Research Abstracts*, 8.
- Kargaranbafghi, F., Neubauer, F., Genser, J., 2010. Mesozoic and Eocene ductile deformation of western Central Iran: from Cimmerian collisional orogeny to Eocene extension and exhumation. In: EGU general assembly conference abstracts, 62-68
- Kargaranbafghi, F., Neubauer, F., Genser, J., 2011. Cenozoic kinematic evolution of southwestern Central Iran: strain partitioning and accommodation of Arabia-Eurasia convergence. *Tectonophysics*, 502(1): 221-243.
- Katja Deckart, K., Clark, A. H., Celso, A. A., Ricardo, V., Bertens, A. N., Mortensen, K. J., Fanning, M., 2005. Magmatic and Hydrothermal Chronology of the Giant Rio Blanco Porphyry Copper Deposit, Central Chile: Implications of an Integrated U-Pb and $^{40}\text{Ar}/^{39}\text{Ar}$ Database. *Economic Geology*, 100 (5): 905-934. <https://doi.org/10.2113/gsecongeo.100.5.905>
- Linnen, R.L., Keppler, H., 2002. Melt composition control of Zr/Hf fractionation in magmatic processes. *Geochimica et Cosmochimica Acta*, 66: 3293-3301.
- Loiselle, M.C., 1979. Characteristics and origin of orogenic granites. *Geological Society of America*, 11: 468.
- Maniar, P. D., Piccoli, P. M., 1989. Tectonic discrimination of granitoids. *Geological Society of America Bulletin*, 101: 635-643.
- Marks, M., Halama, R., Wenzel, T., Markl, G., 2004. Trace element variations in clinopyroxene and amphibole from alkaline to peralkaline syenites and granites: implications for mineral-melt trace-element partitioning. *Chemical Geology*, 211, 185-215.
- Martin, H., Smithies, R.H., Rapp, R., Moya, J.F., Champion, D., 2005. An overview of adakite, tonalite-trondhjemite-granodiorite (TTG), and sanukitoid: relationships and some implications for crustal evolution. *Lithos*, 79: 1-24.
- McCurry, M., Hayden, K.P., Morse, L.H., Mertzman, S., 2008. Genesis of post-hotspot, A-type rhyolite of the eastern Snake River Plain volcanic field by extreme fractional crystallization of olivine tholeiite. *Bulletin of Volcanology*, 70(3): 361-383.
- McDonough, W., Frey, F., 1989. Rare earth elements in upper mantle rocks. *Reviews in Mineralogy and Geochemistry*, 21(1):100-145.
- McQuarrie, N., Stock, J.M., Verdel, C., Wernicke, B.P., 2003. Cenozoic evolution of Neotethys and implications for the causes of plate motions. *Geophysical Research Letters*, 30: 20-36. doi: 10.1029/2003GL017992.
- Mohajjel, M., Fergusson, C.L., Sahandi, M.R., 2003. Cretaceous-Tertiary convergence and continental collision, Sanandaj-Sirjan Zone, western Iran. *Journal of Asian Earth Sciences*, 21: 397-412, doi: 10.1016/S1367-9120(02)00035-4.
- Mousavi Makoui, A., 1998. Petrological study of Narigan granite, master's thesis, Shahid Beheshti University.
- Nik Tabar S.M., Rashidnjademran, N., 2015. Geochemistry and Lithography of Mafic Floods in Rizo Series, North of Bafq (Central Iran). *Geochemistry*, 5(3): 261-267.
- Paulick, H., Bach, W., Godard, M., De, HJCM., Surir, G., Harvey, J., 2006. Geochemistry of abyssal peridotites (Mid-Atlantic Ridge, 15200N, ODP Leg 209): implication for fluid/rock interaction in slow spreading environments. *Chemical Geology*, 234:179-210.
- Pearce, J.A., 1983. Role of the sub-continental lithosphere in magma genesis at active continental margins. In: Hawkesworth CJ, Norry MJ (eds) *Continental basalts and mantle xenoliths*. Shiva Publications, Nantwich, Cheshire, pp 230-249.
- Pearce, J. A., Harris, N.B., Tindle, A.G., 1984. Trace element discrimination diagrams for the tectonic interpretation of granitic rocks. *Journal of Petrology*, 25: 956-983.
- Pollard, D.D., 1987. Elementary fracture mechanics applied to the structural interpretation of dykes. In: Halls, H.C., Fahrig, W.H. (Eds.), *Mafic Dyke Swarms*, vol. 34. Geological Association of Canada Special Paper, pp. 524.
- Prichard, H.M., 1993. *Magmatic Processes and Plate Tectonics* (Geological Society Special Publication No 76). Amer Assn of Petroleum Geologists.

- Prowatke, S., Klemme, S., 2005. Effect of melt composition on the partitioning of trace elements between titanite and silicate melt. *Geochimica et Cosmochimica Acta* 69, 695-709.
- Ramezani, J. and Tucker, R., 2003. The Saghand region, Central Iran: U/Pb geochronology, petrogenesis and implication for Gondwana tectonics. *American Journal of Science* 303: 622-665. <https://doi.org/10.2475/ajs.303.7.622>.
- Robertson, A.H.F., Clift, P.D., Degnan, P.J., Jones, G., 1991. Paleogeographic and paleotectonic evolution of the Eastern Mediterranean Neotethys. *Palaeogeography Palaeoclimatology Palaeoecology*, 87: 289-343.
- Robertson, A.H.F., 2000. Mesozoic-Tertiary tectonic-sedimentary evolution of a south Tethyan oceanic basin and its margins in southern Turkey, in Bozkurt, E., et al., eds., *Tectonics and magmatism in Turkey and the surrounding area: Geological Society [London] Special Publication*, 173: 97-138.
- Rollinson, H.R., 1993. *Using geochemical data: evaluation, presentation, interpretation*. Longman, Harlow, England.
- Rudnick, R.L., Fountain, D.M., 1995. Nature and composition of the continental crust: A lower crustal perspective. *Reviews of Geophysics*, 33: 267-30, <https://doi.org/10.1029/95RG01302>.
- Sarhadi, N., Ahmadi A., Firouzkohi Z. and Jami M., 2016. Lithology and geochemistry of mesocratic and malnocatic dykes in Lakhshak granodiorite body, North West of Zahedan. *104, 26:149-162*.
- Saunders, AD., Norry, MJ., Tarney, J., 1988. Origin of MORB and chemically-depleted mantle reservoirs: trace element constraints. *Journal of Petrology*, 1: 415-445.
- Schndl, E.S., Gorton, M.P., 2002. Application of high field strength elements to discriminate tectonic settings in VMS environments. *Economic geology*, 97(3): 629-642.
- Shelley, D., 1993. *Igneous and metamorphic rocks under the microscope: classification, textures, microstructures and mineral preferred-orientations*.
- Şengör, A.M.C., Kidd, W.S.F., 1979. The post-collisional tectonics of the Turkish- Iranian Plateau and a comparison with Tibet. *Tectonophysics*, 55: 361-376.
- Şengör, A.M.C., Natal'in, B.A., 1996. *Palaeotectonics of Asia: Fragments of a synthesis*: Cambridge University Press, Cambridge.
- Sengor, A.M.C., Cin, A., Rowley, D.B., Nie, S.Y., 1993. Space-time patterns of magmatism along the Tethysides: a preliminary study. *Journal of Geology*, 101: 51-84.
- Stalder, R., Foley, S. F., Brey, G.P. and Horn, I., 1998. Mineral-aqueous fluid partitioning of trace elements at 900-1200°C and 3.0-5.7 GPa: new experimental data for garnet, clinopyroxene, and rutile, and implications for mantle metasomatism. *Bulletin of the Geological Society of America*, 62: 1781-1801.
- Stocklin, J., 1974. Possible ancient continental margins in Iran. In: Burk, C.A., Drake, C.L. (Eds.), *The Geology of Continental Margins*. Springer Verlag, 873-887.
- Stoneley, R., 1981. The Geology of the Kuh-e Dalneshin Area of Southern Iran, and Its Bearing on the Evolution of Southern Tethys. *Journal of the Geological Society*, 138:509-526. <http://dx.doi.org/10.1144/gsjgs.138.5.0509>
- Tajbakhsh, G.H., 2020. Petrography, geochemistry and tectonic setting of mafic dyke swarm of Zargian granitoid, North of Bafq (Central Iran). *Scientific Quarterly Journal*, 30: 175-188.
- Tchameni, R., Pouclet, A., Penay, J., Ganwa, A.A., Toteu, SF., 2006. Petrography and geochemistry of the Ngaondere Pan - African granitoids in Central North Cameroon: Implication for their sources and geological setting. *Journal of African Earth Sciences*, 44: 511 -529.
- Tillman, J. E.A., Poosti, S., Rossello, S., Eckert., A., 1981. Structural evolution of Sanandaj-Sirjan Ranges near Esfahan, Iran. *American Association of Petroleum Geologists*, 65: 674-687p.
- Verdel, C., Wernicke, B.P., Ramezani, J., Hassanzadeh, J., Renne, P.R., Spell, T.L., 2007. Geology and thermochronology of Tertiary Cordilleran-style metamorphic core complexes in the Saghand region of Central Iran. *Bulletin of the Geological Society of America*, 119(7-8): 961-977.
- Vernon, R.H., Clarke, G.L. 2008. *Principles of Metamorphic Petrology*. Cambridge University Press.
- Walker, J.A., Patino, L.C., Carr, M.J., Feigenson, M.D. 2001. Slab control over HFSE depletions in Central Nicaragua. *Earth and Planetary Science Letters*, 192: 533-543.
- Wedepohl, K.H. 1995. The Composition of the Continental Crust. *Geochimica et Cosmochimica Acta*, 59: 1217-1232. [http://dx.doi.org/10.1016/0016-7037\(95\)00038-2](http://dx.doi.org/10.1016/0016-7037(95)00038-2)
- Wilson, M., 1989. *Igneous petrogenesis: a global tectonic approach*. Chapman and Hall, New York, 496 p.

- Wood, D.A., 1980. The application of a Th-Hf-Ta diagram to problems of tectonomagmatic classification and to establishing the nature of crustal contamination of basaltic lavas of the British Tertiary volcanic province. *Earth and Planetary Science Letters*, 42: 77-97.
- Woodruff, F., Savin, S.M., 1989. Miocene deep water oceanography. *Paleoceanography* 4, 87-140.
- Xu, Y.G., Lan, J.B., Yang, Q.J., Huang, X.L., Qiu, H.N., 2008. Eocene break-off of the NeoTethyan slab as inferred from intraplate-type mafic dykes in the Gaoligong orogenic belt, eastern Tibet. *Chemical Geology*, 255: 439-453.
- Yadav, P., Sarma, D.S., 2021. Geochemistry of 2.21 Ga giant radiating dyke swarm from the Western Dharwar Craton, India: Implications for petrogenesis and tectonic evolution. *Geological Journal*, 1-26.
- Yang, Q.Y., Santosh, M., Dong, G., 2014. Late Palaeoproterozoic post-collisional magmatism in the North China Craton: geochemistry, zircon U-Pb geochronology, and Hf isotope of the pyroxenite-gabbro-diorite suite from Xinghe, Inner Mongolia. *International Geology Review*, 56: 959-984.
- Yazdani, M., Masoumeh Ahangari, M., Jahangiri, A., Shokohi, H., 2016. Petrology and geochemistry of Nabijan gabbroic and dioritic plutons (southwest Kaleybar, NW Iran): an implication for post-collision magmatism. *Petrology* 7(26): 1-22.
- Yazdi, A., Ashja-Ardalan, A., Emami, M.H., Dabiri, R., Foudazi, M., 2019. Magmatic interactions as recorded in plagioclase phenocrysts of quaternary volcanics in SE Bam (SE Iran), *Iranian Journal of Earth Sciences*, 11(3): 215-224. <https://doi.org/10.30495/ijes.2019.667379>
- Yazdi, M. Rasa, A. Nooryan Ramsheh, Z. Librarian, M. and Baskabadi, A., 2013. Albit formation in igneous rocks of Chah-Jole area, *Journal of Basic Sciences of Islamic Azad University*, edition, 21 pages.
- Yılmaz, Y., 1993. New evidence and model on the evolution of the southeast Anatolian Orogen. *Geological Society of America Bulletin*, 105: 251-71.
- Zhang, Z.C., Mahoney, J.J., Mao, J.W., Wang, F.H., 2006. Geochemistry of picritic and associated basalt flows of the western Emeishan flood basalt province, China. *Journal of Petrology*, 47 (10): 1997-2019.

